Fluctuation-induced diamagnetism above the superconducting transition in MgB_2

J. Mosqueira, M. V. Ramallo, S. R. Currás, C. Torrón, and F. Vidal
Laboratorio de Baixas Temperaturas e Superconductividade (Unidad Asociada al Consejo Superior de Investigaciones Científicas, Spain) (LBTS), Departamento de Física da Materia Condensada, Universidade de Santiago de Compostela E15782, Spain
(Received 16 November 2001; revised manuscript received 14 February 2002; published 2 May 2002)

The behavior of the superconducting fluctuations in the normal state in MgB_2 is studied through measurements of the fluctuation-induced diamagnetism (FD). These experiments show that the superconducting fluctuations in this compound are three dimensional in nature. Moreover, for reduced magnetic fields up to 0.5 the FD is not appreciably affected by nonlocal electrodynamic effects. This last FD behavior is in striking contrast with the one always observed, at equivalent reduced magnetic fields, in all other clean low-temperature metallic superconductors studied until now, but it is similar to the one found in cuprate superconductors. A sharp decrease of the fluctuation effects is observed around $\varepsilon = \ln(T/T_C) \approx 0.6$, in agreement with recent results obtained in other low-T_C and high-T_C superconductors. This last result confirms the need of a total-energy cutoff condition to extend the applicability of the Gaussian-Ginzburg-Landau approach to the high reduced-temperature region.

DOI: 10.1103/PhysRevB.65.174522 PACS number(s): 74.40.+k, 74.20.De, 74.25.Ha, 74.70.Ad

I. INTRODUCTION

The recent discovery of superconductivity in MgB_2 has generated an intense research activity, mainly due to its high critical temperature ($T_C \approx 40$ K) compared to the conventional low-temperature superconductors (LTSC's).[1,2] The interest in this compound is enhanced by the fact that other fundamental characteristics [as the superconducting coherence length amplitude $\xi(0)$, the Ginzburg-Landau (GL) parameter κ, or the anisotropy factor γ] are halfway between those of the LTSC's and of the high-temperature cuprates (HTSC's).[1,2] In this paper we address the superconducting fluctuation effects, associated with the presence of Cooper pairs created by thermal fluctuations above T_C, in MgB_2. For that we present measurements of the decrease of the magnetization above T_C due to the presence of these fluctuating Cooper pairs in a randomly oriented polycrystalline sample. This effect, called fluctuation-induced diamagnetism (FD), was chosen because it provides direct information on the superconducting fluctuations in the normal state and, simultaneously, it is relatively easy to study in randomly oriented polycrystalline samples. In addition, at present there exist detailed FD measurements in different LTSC's (Refs. 3 and 4), and HTSC (Refs. 5 and 6), which will then allow interesting comparisons. For instance, it is worthwhile to wonder whether due to the layeredlike crystallographic structure of MgB_2 its fluctuations are two dimensional (2D) in nature, like in the HTSC's, or instead they are three dimensional (3D) as is the case of most conventional LTSC's.[3] Two other interesting questions are the possible influence of nonlocal electrodynamic effects[3,4,7] and the influence of short-wavelength fluctuations which may be particularly important at high reduced temperatures, when $\xi(T)$ becomes of the order of $\xi(0)$.[3,4,8,9] The nonlocal effects on the superconducting fluctuations are important in clean LTSC's,[3,4,7] but they are unobservable in the case of extremely type-II HTSC's.[8,9] In addition to their relevance when analyzing the thermal fluctuations, these effects may concern other central magnetic properties, such as vortex pinning or even the nature itself of the flux line lattice.[10,11] Concerning short-wavelength fluctuation effects at high reduced temperatures [for $\varepsilon \equiv \ln(T/T_C) \geqslant 0.1$], they have been already observed in both HTSC's (see Refs. 8 and 9 and references therein) and LTSC's.[3,4] Moreover, it has been observed in the last two years that the superconducting fluctuation effects vanish at a well-defined temperature given by $T^C \approx 1.7 T_C$.[4,8,9] This striking result has been recently attributed to the limits imposed by the uncertainty principle to the shrinkage, when the temperature increases, of the superconducting wave function.[4,12] MgB_2, which as noted before has superconducting parameters well between those of the HTSC's and LTSC's [mainly $\xi(0)$ and κ], is particularly suited to probe the universality of this high-ε behavior of the superconducting fluctuations.

II. EXPERIMENTAL DETAILS AND RESULTS

In the present experiments we used a commercial (Alfa, 99.9% purity) polycrystalline sample of MgB_2 with a mass of 0.50 g. Such a big sample, which has a volume near the maximum of our measurement system [a superconducting quantum interference device (SQUID) magnetometer, Quantum Design, model MPMS], is necessary in order to have resolution enough to measure the fluctuation magnetization in the high-reduced-temperature region (see below). Due to the small anisotropy of this compound, it was not possible to align the grains magnetically and, thus, we used a randomly oriented sample (x-ray analyses confirmed that it had no preferable orientation). Various examples of the as-measured magnetization as a function of temperature at constant applied magnetic fields, $M(T)_H$, are presented in Fig. 1(a). The lines are the normal-state or background contribution, $M_B(T)_H$, which were obtained by fitting a degree-2 polynomial in a temperature region above $\sim 2T_C$ and up to $\sim 3.5T_C$, where the fluctuation effects are expected to be negligible. Such a function fits very well the data in the background region (the regression factor r was better than 0.999) and it extrapolates smoothly through the transition. The inclusion of higher-degree terms does not improve r substantially. We discarded more physical (Curie-like) func-

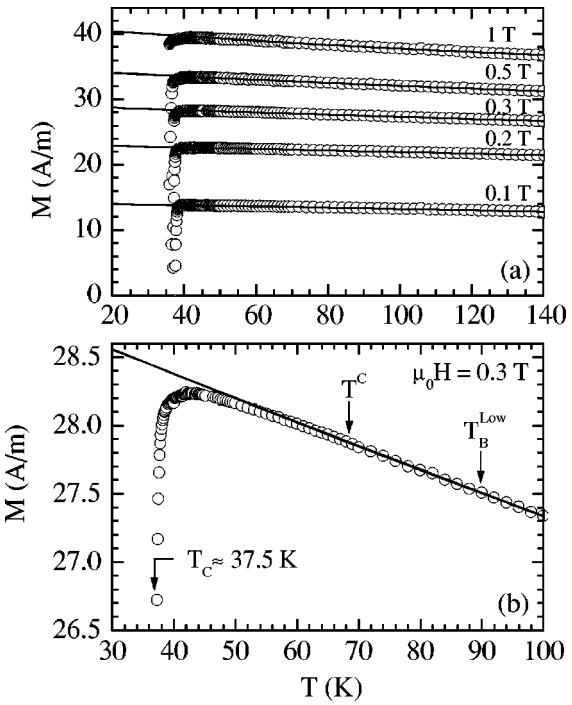

FIG. 1. (a) Some examples of the as-measured magnetization vs temperature curves at constant applied magnetic fields. The solid lines are the backgrounds, which were obtained by fitting a degree-2 polynomial in different temperature regions that always were inside $2<T/T_C<3.5$. (b) Details near T_C of the $M(T)_H$ curve corresponding to $\mu_0 H=0.3$ T. In this example, the background fitting region was bounded by 90 K$\leqslant T\leqslant$130 K. Its lower limit, noted T_B^{Low}, is indicated in this figure, together with the temperature T^C at which the FD vanish.

tions because they fitted worse. This is not surprising because the measured magnetic moments have a non-negligible contribution of the sample holder (which includes a gelatin capsule with a piece of adhesive tape). The temperature at which $M(T)_H$ becomes indistinguishable from the background is denoted as T^C [see Fig. 2(b)]. This last temperature is not appreciably affected by the choice of the background fitting region provided that it is above $2T_C$ and up to $3.5T_C$ (see the next section).

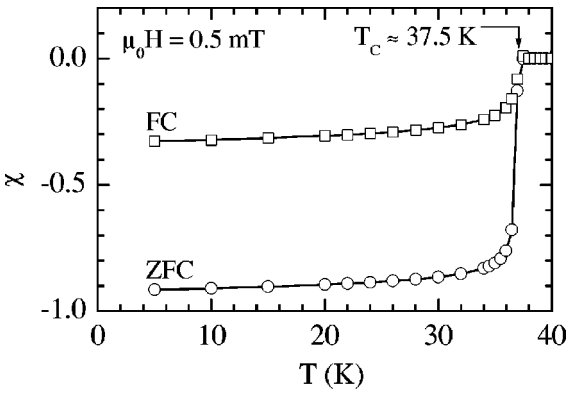

FIG. 2. Temperature dependence of the low-field magnetic susceptibility measured under field-cooled and zero-field-cooled conditions. The lines are guides for the eyes.

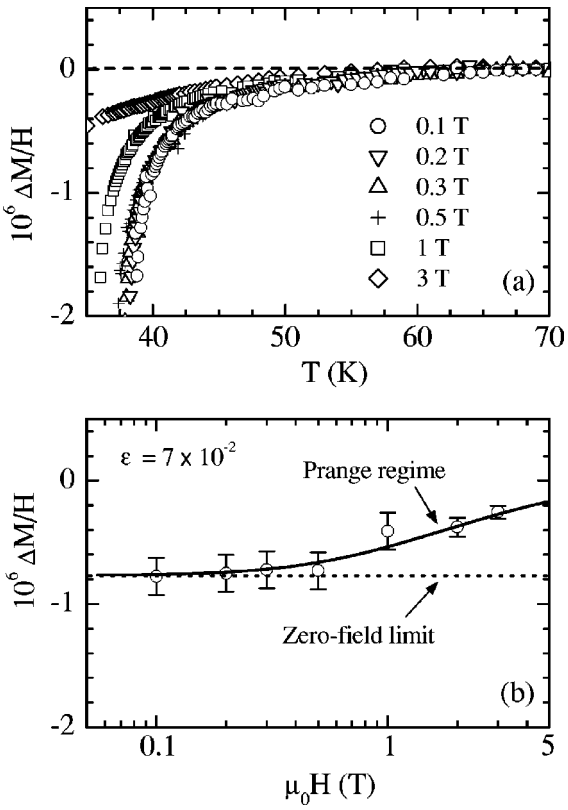

FIG. 3. (a) Some examples of the temperature dependence of the excess magnetization (over H). (b) Magnetic field dependence of the excess magnetization at a constant temperature. The solid line is the angular-averaged finite-field GGL approach, while the dotted line corresponds to the *H*-independent zero-field limit.

The field-cooled (FC) and zero-field-cooled (ZFC) magnetic susceptibilities are presented in Fig. 2. These data were obtained by using an external magnetic field of 0.5 mT, which is smaller than the lower critical magnetic fields (at least for temperatures not very close to T_C). The as-measured data were corrected for demagnetizing effects by assuming that the grains are spherical and that the magnetic flux trapping and shielding are isotropic in this Meissner region.[13] The resulting χ^{ZFC} is near -1 at low temperatures, as expected for complete magnetic shielding and justifying the spherical approximation. However, χ^{FC} is near -0.3, a value which may be attributed to magnetic flux trapped by structural inhomogeneities and nonsuperconducting domains in the sample grains. The transition temperature ($T_C \approx 37.5$ K) was determined from the onset of the diamagnetic transition. The transition width of the ZFC or FC curves is of the order of $\Delta T_C \approx 0.8$ K. Although relatively narrow, this transition width may be in turn attributed to stoichiometric inhomogeneities like, in particular, those related to isotope effects due to the presence in commercial MgB_2 of the boron isotopes ^{10}B and ^{11}B in the natural proportions ($\sim$19% and $\sim$81% respectively).[14,15] To elude the effect of these T_C inhomogeneities, we will restrict the analysis to $T\gtrsim T_C+0.8$ K, which corresponds to reduced temperatures $\varepsilon\equiv\ln(T/T_C)\gtrsim 2\times10^{-2}$.

Various examples of the temperature dependence of the so-called fluctuation-induced magnetization, $\Delta M(T)_H$, for

the different applied magnetic fields and for temperatures around T_C, are presented in Fig. 3(a). As usually, $\Delta M(T,H)$ is defined as $\Delta M(T,H) \equiv M(T,H) - M_B(T,H)$. These data have been normalized by their corresponding H amplitudes. This figure already illustrates at a qualitative level one of the central aspects of our paper: the $\Delta M(T)_H$ curves corresponding to the lowest applied magnetic fields agree with each other, even for temperatures close to T_C; i.e., they are H independent. This may be better seen in Fig. 3(b), where $\Delta M/H$ is represented as a function of the external magnetic field at a constant temperature above T_C. The field independence of the susceptibility is the behavior predicted by Gaussian-Ginzburg-Landau (GGL) theory in the so-called zero-magnetic-field (or Schmidt-Schmid) limit[16] (see also below). This provides then a direct indication of the absence of finite-field (or Prange) effects but also of appreciable nonlocal electrodynamic effects for $\mu_0 H \lesssim 0.3$ T.[3,4,7] Above $\mu_0 H \approx 0.5$ T the data separate from the zero-field limit but they may be explained by just taking into account the conventional (or Prange) finite-field effects (see the next section). This last result extends the absence of nonlocal effects at least up to 3 T. As commented on above, such a behavior of $\Delta M(T)_H$ at low-field amplitudes is characteristic of HTSC's[5,6,8] and it has also been observed recently in a dirty LTSC alloy.[4] However, MgB_2 is well in the clean limit[17] and, therefore, it is the first time that the FD in the zero-field limit is observed in a clean noncuprate superconductor. The absence of appreciable nonlocal effects at low-field amplitudes in MgB_2, in spite of the clean character of this compound, may be attributed to its relatively high Ginzburg-Landau parameter $\kappa \approx 10$ (see below) when compared to conventional LTSC's.[3,7]

III. ANALYSIS AND DISCUSSION

A more quantitative comparison between the experimental results and the GGL approach may be done through the reduced-temperature dependence of the excess magnetization (normalized to HT). The data shown in Fig. 4(a) correspond to the lowest magnetic field amplitudes used in our present experiments. As can be seen, the $\Delta M/HT$ versus ε curves obtained for different field amplitudes agree with each other in the entire measured ε range. These results fully confirm, therefore, our conclusions summarized above on the penetration in the zero-field limit and on the absence of appreciable nonlocal effects on the FD in MgB_2.

To analyze the data of Fig. 4(a) on the grounds of the GGL approach we may start by comparing with the zero-magnetic-field limit without any cutoff. For a polycrystalline sample with anisotropic 3D grains randomly oriented, $\Delta M(\varepsilon)_H$ may be obtained by angular averaging, following the standard procedure (see, e.g., Ref. 13), the fluctuation magnetization of a single grain.[16,18] This leads to

$$\frac{\Delta M}{HT}(\varepsilon) = -\frac{\pi \mu_0 k_B \xi_{ab}(0)}{6\phi_0^2}\left(\frac{\gamma}{3}+\frac{2}{3\gamma}\right)\varepsilon^{-1/2}, \qquad (1)$$

where $\xi_{ab}(0)$ is the coherence length amplitude in the ab crystallographic plane, ϕ_0 the flux quantum, μ_0 the vacuum permeability, and k_B the Boltzmann constant. The dot-dashed line in Fig. 4(a) is a fit of Eq. (1) to the data near T_C (up to $\varepsilon \approx 7\times 10^{-2}$) where the short-wavelength effects are expected to be negligible. In doing this fit the temperature-independent prefactor in Eq. (1) is the only free parameter.

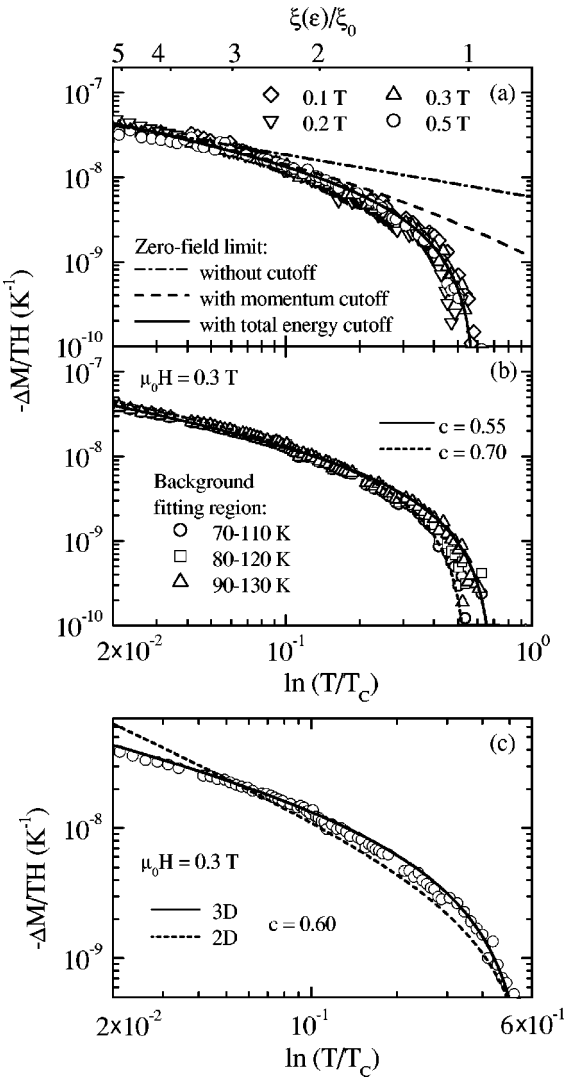

FIG. 4. (a) ε dependence of the fluctuation-induced magnetization (over HT) for different applied magnetic fields. The curves correspond to the GGL approach for anisotropic 3D superconductors in the zero-field limit under different cutoff conditions. The $\xi(\varepsilon)/\xi_0$ scale, which numerical values correspond to the BCS clean limit, illustrates how the behavior of the fluctuation-induced magnetization is dominated by the localization energy when the superconducting coherence length competes with ξ_0, the actual (or Pippard) coherence length at $T=0$ K. (b) $-\Delta M(\varepsilon)/HT$ curves for $\mu_0 H = 0.3$ T, obtained by using different background fitting regions. The lines represent again the GGL approach in the zero-field limit under a total-energy cutoff. The corresponding cutoff amplitudes vary only between 0.55 and 0.7. (c) Comparison between the 3D and the 2D limits of the low-field GGL approaches and the experimental data for $\mu_0 H = 0.3$ T. The 2D limit disagrees with the reduced-temperature dependence of the experimental data. Moreover, its amplitude is very different from the one that may be obtained from the coherence length values (see the main text for details). In (a) and (c) the background fitting region was $\sim$80–120 K.

As may be observed, up to $\varepsilon \approx 8\times10^{-2}$ the measured FD follows the $\varepsilon^{-1/2}$ dependence typical of 3D fluctuations. Although the ε region ($2\times10^{-2} \leqslant \varepsilon \leqslant 8\times10^{-2}$) is relatively narrow, such a comparison provides already a first indication of the 3D nature of the superconducting fluctuations in MgB_2. We will see below that the introduction of a cutoff condition will allow us to extend this dimensionality analysis up to 5×10^{-1}. This last analysis will also confirm the 3D character of the superconducting fluctuations in MgB_2. This result is consistent with the fact that in this compound the coherence length amplitudes are in all directions at least one order of magnitude larger than the corresponding unit cell lengths and also much smaller than the individual grain sizes: from measurements of the H dependence of the reversible mixed-state magnetization and taking $\gamma = 1.7$–2.6,[2] we obtained $\xi_{ab}(0) = 73 \pm 2$ Å and $\xi_c(0) = \xi_{ab}(0)/\gamma = 36 \pm 8$ Å (see the Appendix).

In what concerns the FD amplitude, by using those $\xi_{ab}(0)$ and γ values in Eq. (1) one finds that the theoretical amplitude is around a factor of 2.7 larger than the measured one. This amplitude difference, which was also observed in HTSC's,[5,13] may be attributed to structural inhomogeneities with characteristic lengths of the order of or somewhat larger than the coherence lengths values. This is consistent with the fact that the Meissner fraction is reduced from its ideal value in the same amount (see Fig. 2). In fact, the experimental FD amplitude regularized through the Meissner fraction is found to be in excellent agreement with the theoretical one for 3D anisotropic superconductors [and using in Eq. (1) the parameter values obtained in the Appendix; see also below].

One may also see in Fig. 4(a) that for $\varepsilon \geqslant 0.1$ the measured FD falls off much rapidly than predicted by the conventional mean-field behavior, and it vanishes above a well-defined reduced temperature ε^C close to 0.6. This FD behavior at high reduced temperatures has been already observed in different HTSC and LTSC and, as noted before, it has been attributed to the limits imposed by the uncertainty principle to the shrinkage of the superconducting wavefunction when the reduced-temperature increases.[4,8,12] On the grounds of the GGL approach, these ideas may be taken into account by introducing a so-called ''total-energy'' cutoff condition,[4,8,12] which could extend the applicability of this mean field approach from $\varepsilon \ll 1$ up to high reduced temperatures (see also Ref. 19). To probe the adequacy of such a regularization of the GGL approach in MgB_2 is another aim of the present paper.

The FD in anisotropic bulk superconductors may be straightforwardly calculated on the grounds of the GGL approach under different cutoff conditions by just extending to this case our recent GGL results in isotropic superconductors.[4] Under the total-energy cutoff this leads to

$$\Delta M_{ab}(T,H,c) = -\frac{k_B T \mu_0 H \gamma \xi_{ab}(0)}{3\phi_0^2} \times \left(\frac{\arctan\sqrt{(c-\varepsilon)/\varepsilon}}{\sqrt{\varepsilon}} - \frac{\arctan\sqrt{(c-\varepsilon)/c}}{\sqrt{c}} \right), \tag{2}$$

and $\Delta M_c(T,H,c) = \Delta M_{ab}(T,H,c)/\gamma^2$, where $c \leqslant 1$ is the cutoff amplitude, which in the absence of nonlocal effects may be approximated as a constant. The corresponding expressions under the conventional momentum a cutoff may be easily obtained by just changing c by $c+\varepsilon$. Note also that this expression includes the one without cutoff as a limiting case, which corresponds to $\varepsilon \ll c$. Again, the FD measured in a randomly oriented polycrystalline sample is given by the angularly averaged expression

$$\frac{\Delta M}{HT}(\varepsilon,c) = \left(\frac{1}{3} + \frac{2}{3\gamma^2} \right) \frac{\Delta M_{ab}}{HT}(\varepsilon,c). \tag{3}$$

The solid line in Fig. 4(a) is the best fit of Eq. (3) to the data in the low-magnetic-field limit (i.e., for $\mu_0 H \leqslant 0.5$ T and $\varepsilon \geqslant 2\times10^{-2}$), with the temperature-independent amplitude and c as free parameters. As can be seen, the agreement is excellent in all the experimentally accessible ε region (including the high-reduced-temperature region above 0.1) and it leads to $c \approx 0.6$, whereas the amplitude is 0.48 times the theoretical one, this factor being again close to the Meissner fraction. For completeness, we also show in Fig. 4(a) a similar comparison with the theoretical FD under a momentum cutoff (dashed line), evaluated by using the same c value and FD amplitude. As expected, in this case the agreement is reasonable only below $\varepsilon \approx 0.2$. The failure at higher reduced temperatures could be corrected by using a lower value of c, but this would then break the agreement for $\varepsilon \leqslant 0.1$. The total-energy cut off reproduces well both the FD behavior below ε^C and the vanishing at $\varepsilon^C = c$.

A check of the influence of the background region choice on the extracted FD is shown in Fig. 4(b). This example corresponds to the data obtained under $\mu_0 H = 0.3$ T. The background fitting region was always taken between $1.9 \leqslant T/T_C \leqslant 3.5$. As may be clearly seen, the resulting ε^C values spread from 0.55 to 0.70, but the experimental data may be equally well fitted by the total-energy cutoff approach taking c values in that range. Let us also point out that the ε^C value is almost independent of the applied magnetic field and, at least up to $\mu_0 H = 3$ T, it remains close to 0.6.

The fact that the ε^C value found in MgB_2 is similar to the one found in clean 2D and 3D HTSC's,[8,9] and in dirty 3D LTSC alloys[4] provides a further confirmation of the fundamental origin of such a behavior of the thermal fluctuations at high reduced temperatures. In addition, the ε^C value agrees with the one which may be directly estimated for clean BCS superconductors by defining ε^C through $\xi(\varepsilon^C) = \xi_0$ and using the mean-field ε dependence of $\xi(\varepsilon)$ and $\xi(0) = 0.74\xi_0$.[4,12] Here ξ_0 is the actual (or Pippard) superconducting coherence length at $T = 0$ K. The $\xi(\varepsilon)/\xi_0$ scale in Fig. 4(a) (which numerical values correspond to the BCS clean limit) shows that when $\xi(\varepsilon) \geqslant 2\xi_0$, which roughly correspond to $\varepsilon \leqslant 0.15$, the consequences of the localization energy contribution to the total-energy cutoff [the term proportional to $1/\xi^2(\varepsilon)$; see Refs. 4, 8 or 9] on the FD are unappreciable. However, for $2\xi_0 \geqslant \xi(\varepsilon) \geqslant \xi_0$ (corresponding to $0.15 \geqslant \varepsilon \geqslant \varepsilon^C$), i.e., when the superconducting coherence length competes with the size of the individual Cooper pairs, the uncertainty principle will dominate the behavior of these Cooper pairs.

For completeness, in Fig. 4(c) we present a comparison of the 3D and 2D limits of the GGL approach in the zero-field regime with the experimental data. In doing that comparison the absolute amplitude was in both limits a free parameter. As is clearly seen, the ε behavior of the GGL approach in the 2D limit strongly disagrees with the reduced-temperature dependence of the experimental data. But, in addition, the theoretical amplitude obtained by using the coherence length values in the Appendix is over one order of magnitude larger than the experimental amplitude.[8] Such a discrepancy is too big to be attributed to inhomogeneity effects.

Let us finally analyze the H dependence of the FD in the finite-field regime. As commented on above, for fields larger than 0.5 T the $\Delta M(T)_H/H$ amplitude decreases appreciably, mainly close to T_c, well below the one measured in the zero-field limit. In Fig. 3(b) is presented a comparison of the $\Delta M(H)_T/H$ data with the GGL approach in the finite-field (or Prange) regime (solid line). It was obtained by generalizing the 3D isotropic result in the finite-field regime[4] to the anisotropic case (through the scaling transformation suggested in Ref. 18) and then performing the angular average. As is clearly seen, the agreement with the experimental data is excellent, thus extending the applicability of the GGL approach up to the highest magnetic fields studied ($\mu_0 H = 3$ T). This last result discards the presence of appreciable nonlocal electrodynamic effects up to a considerable fraction of the upper critical magnetic field [$H/H_{c2}^{\perp}(0) \sim 0.5$].

IV. CONCLUSIONS

In conclusion, the fluctuation induced diamagnetism in MgB_2 was measured as a function of the applied magnetic field (up to $\mu_0 H = 3$ T) and of the reduced temperature (for $2\times10^{-2} \leqslant \varepsilon \leqslant 1$). For $\mu_0 H \lesssim 0.3$ T the FD is H independent at all accessible reduced temperatures. This shows that these data correspond to the so-called zero-magnetic-field (or Schmidt-Schmid) limit and that the nonlocal electrodynamic effects are irrelevant in MgB_2 up to these magnetic field amplitudes. Our results also suggest that for higher reduced magnetic fields the decrease of the FD may be explained by taking into account the conventional (Prange) finite-field effects. This extends up to $H/H_{c2}^{\perp}(0) \sim 0.5$ the absence of appreciable nonlocal effects. In the light of recent results in other superconductors,[10,11] this behavior could have implications in the vortex pinning and in the structure of the flux line lattice in MgB_2. These particular characteristics of MgB_2, when combined with presumably enhanced vortex fluctuations due to its relatively high T_C, suggest that the MgB_2 could be a good candidate to observe the unusual vortex lattice effects recently reported in borocarbides.[10] For $\varepsilon \leqslant 8\times10^{-2}$, the data in the low-field limit follow at a quantitative level the critical exponent and amplitude of the GGL approach in the 3D limit. The 3D nature of the superconducting fluctuations in MgB_2 is further confirmed by extending the FD analysis to the high-reduced-temperature region (up to $\varepsilon \approx 0.5$) by regularizing the GGL approach through a total-energy cutoff. Such a total-energy cutoff also accounts for the vanishing of the FD at a well-defined reduced temperature $\varepsilon^C \approx 0.6$. Our present results confirm, therefore, the deep influence of the confinement energy arising from the shrinkage of the superconducting wave function on the superconducting fluctuations at high reduced temperatures.

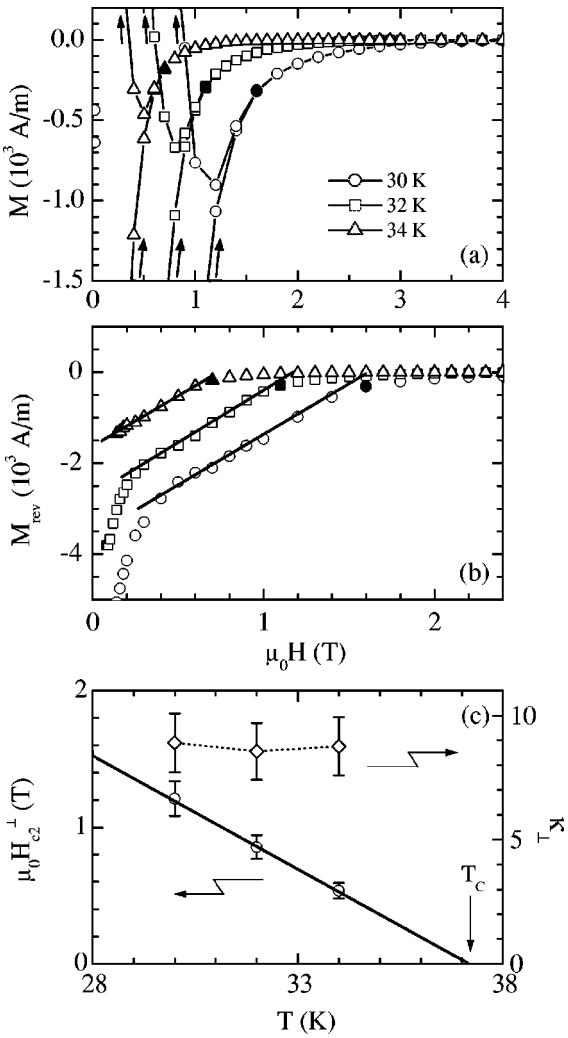

FIG. 5. (a) Some examples of the magnetization vs external magnetic field curves obtained at some constant temperatures below T_C. A small paramagnetic contribution has been already subtracted from these curves. The solid symbol in each curve corresponds to the magnetic field below which the magnetization is irreversible. (b) Reversible contribution to the magnetization, obtained as the semisum of the data measured by increasing and, respectively, decreasing the applied magnetic field. The solid lines are fits to the angular averaged Abrikosov theory [Eq. (A2)] to the data in the linear region. The resulting $H_{c2}^{\perp}(T)$ and $\kappa_{\perp}(T)$ values are shown in (c), where the error bars come from the uncertainty in the value of the anisotropy factor ($1.7 \leqslant \gamma \leqslant 2.6$).

ACKNOWLEDGMENTS

This work has been financed by Xunta de Galicia (PGIDT01PXI20609PR), the CICYT (MAT2001-3272), and Unión Fenosa (Contract No. 0666-98) Spain.

APPENDIX: DETERMINATION OF THE COHERENCE LENGTH AMPLITUDES FROM MAGNETIZATION MEASUREMENTS BELOW T_C

In order to determine the central superconducting parameters used in the analysis of the fluctuation-induced diamagnetism presented in this paper, we performed $M(H)_T$ measurements of the magnetization versus magnetic field curves at different temperatures below the transition. Some results are shown in Fig. 5(a), where a small normal-state contribution has been already subtracted. As may be clearly seen, the magnetization is highly irreversible below a well-defined magnetic field $H_{irr}(T)$. This restricts the comparison with the theory to the very narrow region corresponding to $H > H_{irr}(T)$. To overcome this difficulty we approximated the *reversible* magnetization through $M_{rev}=(M^+ + M^-)/2$, where M^+ and M^- are the magnetization obtained when increasing and, respectively, decreasing the external magnetic field. In Fig. 5(b) we present the results for M_{rev} corresponding to the M^+ and M^- data points of Fig. 5(a). $M_{rev}(H)_T$ presents a linear behavior over a wide region, which is consistent with the Abrikosov prediction for the magnetization in the high-field regime.[20] The appreciable rounding for $H \gtrsim H_{irr}(T)$ may be attributed to the anisotropic character of this compound:[2] each individual grain in the sample has an upper critical magnetic field depending on its orientation with respect to the external magnetic field.

To compare these data with the theory, we first angular averaged (through a standard procedure[13]) the magnetization of an individual grain with its *c* crystallographic axis forming an angle θ with respect to the external magnetic field. This last is given by[20,18]

$$M(\theta)=\frac{H-H_{c2}(\theta)}{\beta_A[2\kappa^2(\theta)-1]}, \tag{A1}$$

where $H_{c2}(\theta)=H_{c2}^{\perp}(\cos^2\theta+\gamma^{-2}\sin^2\theta)^{-1/2}$, $\kappa(\theta)=\kappa_{\perp}(\cos^2\theta+\gamma^{-2}\sin^2\theta)^{-1/2}$, $H_{c2}^{\perp}$ and $\kappa_{\perp}$ are, respectively, the upper critical magnetic field and the Ginzburg-Landau parameter corresponding to the $\theta=0$ direction and $\beta_A=1.16$. The resulting angularly averaged magnetization is linear with H for $H<H_{c2}^{\perp}$, and for $\kappa_{\perp}^2 \gg 1$ (as is the case for MgB_2; see below) may be approximated by

$$M=\frac{1}{\beta_A\kappa_{\perp}^2}\left[H\frac{2+\gamma^2}{6\gamma^2}-H_{c2}^{\perp}\left(\frac{1}{4}+\frac{\ln(\sqrt{\gamma^2-1}+\gamma)}{4\gamma\sqrt{\gamma^2-1}}\right)\right]. \tag{A2}$$

The solid lines in Fig. 4(b) are the best fits of Eq. (A2) to the $M_{rev}(H)_T$ curves in the linear region, by using $\kappa_{\perp}$ and $H_{c2}^{\perp}$ as free parameters and $\gamma=1.7$–2.6 (see Ref. 2). The resulting values for $H_{c2}^{\perp}$ and $\kappa_{\perp}$ are shown in Fig. 5(c). H_{c2} is practically linear in the temperature range studied. The extrapolation to $T=0$ K leads to $\mu_0 H_{c2}^{\perp}(0)\sim 6.2\pm 0.3$ T, a value in excellent agreement with the one measured in single crystals.[2] By using the standard relation $\mu_0 H_{c2}^{\perp}(0)=\phi_0/2\pi\xi_{ab}^2(0)$, we determined $\xi_{ab}(0)=73\pm 2$ Å. Finally, the Ginzburg parameter is almost temperature independent near T_C and its value is $\kappa_{\perp}=9\pm 1$.

[1] J. Nagamatsu, N. Nakagawa, T. Muranaka, Y. Zenitani, and J. Akimitsu, Nature (London) **410**, 63 (2001).

[2] For a review see, e.g., C. Buzea and T. Yamashita, Supercond. Sci. Technol. **14**, R115 (2001).

[3] For a review see, e.g., W.J. Skocpol and M. Tinkham, Rep. Prog. Phys. **38**, 1049 (1975).

[4] J. Mosqueira, C. Carballeira, and F. Vidal, Phys. Rev. Lett. **87**, 167009 (2001). See also C. Carballeira, J. Mosqueira, M.V. Ramallo, J.A. Veira, and F. Vidal, J. Phys.: Condens. Matter **13**, 9271 (2001).

[5] For a review see, e.g., F. Vidal and M.V. Ramallo, in *The Gap Symmetry and Fluctuations in High Tc Superconductors*, edited by J. Bok, G. Deutscher, D. Pavuna, and S.A. Wolf (Plenum, London, 1998), p. 477.

[6] C. Carballeira, J. Mosqueira, A. Revcolevschi, and F. Vidal, Phys. Rev. Lett. **84**, 3157 (2000).

[7] J.P. Gollub, M.R. Beasley, R. Callarotti, and M. Tinkham, Phys. Rev. B **7**, 3039 (1973).

[8] J. Mosqueira, C. Carballeira, M.V. Ramallo, C. Torrón, J.A. Veira, and F. Vidal, Europhys. Lett. **53**, 632 (2001).

[9] C. Carballeira, S.R. Currás, J. Viña, J.A. Veira, M.V. Ramallo, and F. Vidal, Phys. Rev. B **63**, 144515 (2001).

[10] V.G. Kogan, A. Gurevich, J.H. Cho, D.C. Johnston, Ming Xu, J.R. Thompson, and A. Martynovich, Phys. Rev. B **54**, 12 386 (1996): A. Gurevich and V.G. Kogan, Phys. Rev. Lett. **87**, 177009 (2001).

[11] A.V. Silhanek, J.R. Thompson, L. Civale, D. McK. Paul, and C.V. Tomy, Phys. Rev. B **64**, 012512 (2001).

[12] F. Vidal, C. Carballeira, S.R. Currás, J. Mosqueira, M.V. Ramallo, and J.A. Veira, cond-mat/0112486 (unpublished).

[13] See, e.g., J. Mosqueira, M.V. Ramallo, A. Revcolevschi, C. Torrón, and F. Vidal, Phys. Rev. B **59**, 4394 (1999).

[14] S.L. Bud'ko, G. Lapertot, C. Petrovic, C.E. Cunningham, N. Anderson, and P.C. Canfield, Phys. Rev. Lett. **86**, 1877 (2001).

[15] These T_C inhomogeneities, of the order of 0.8 K, do not allow an analysis of the fluctuation effects in the temperature region between T_C and $T_C+0.8$ K, and they make still more unrealistic any direct extrapolation to T_C of the experimental results (in addition, in this compound and for low magnetic fields so close to the transition one may penetrate in the full-critical, non-Gaussian region). For a review of the inhomogeneity effects on the thermal fluctuations near T_C see, e.g., F. Vidal, J.A. Veira, J. Maza, J. Mosqueira, and C. Carballeira, *Materials Science, Fundamental Properties and Future Electronic Applications of High-Tc Superconductors*, NATO ASI series, edited by S.L. Dreschler and T. Mishonov (Kluwer-Dordrech, Amsterdam, 2001), p. 289.

[16] H. Schmidt, Z. Phys. **43**, 336 (1968). See also A. Schmid, Phys. Rev. **180**, 527 (1969).

[17] See, e.g., P.C. Canfield, D.K. Finnemore, S.L. Bud'ko, J.E. Ostenson, G. Lapertot, C.E. Cunningham, and C. Petrovic, Phys. Rev. Lett. **86**, 2423 (2001).

[18] R. A. Klemm and J.R. Clem, Phys. Rev. B **21**, 1868 (1980). See also A. Buzdin and D. Feinberg, Physica C **220**, 74 (1994).

[19] As already stressed in Refs. 4 and 8, the short-wavelength effects on the FD were early addressed beyond the conventional momentum cutoff approach in various theoretical papers in the case of the low-T_C superconductors. See, e.g., B.R. Patton, V. Ambegaokar, and J.W. Wilkins, Solid State Commun. **7**, 1287 (1969); P.A. Lee and M.G. Payne, Phys. Rev. Lett. **26**, 1537 (1971); J. Kurkijärvi, V. Ambegaokar, and G. Eilenberger, Phys. Rev. B **5**, 868 (1972). However, as explained in some detail in Refs. 4 and 8, these approaches do not take into consideration the limitations imposed by the uncertainty principle to the superconducting wave function, which effects are dominant at high ε. In the case of the microscopic calculations by Lee and co-workers and of Kurkijärvi and co-workers, these authors use approximations which fail when studying the high-energy fluctuation modes (although they are very useful to study the nonlocal effects; see, e.g., Refs. 3 and 7), as is analyzed in detail in the Comment by B.R. Patton and J.W. Wilkins, Phys. Rev. B **6**, 4349 (1972). The Patton and Wilkins criticism applies also to the works on the paraconductivity at high-ε by L.G. Aslamazov and A.A. Varlamov, J. Low Temp. Phys. **38**, 223 (1980); and by M.R. Cimberle *et al.*, Phys. Rev. B **55**, R14 745 (1997). In the case of the alternative approach due to Patton and co-workers, they introduced an *ad hoc* penalization (not a cutoff) of the fluctuation modes, which in spite of being dependent on the total energy was not constructed to take into account the uncertainty principle. As a result, the approaches proposed in all these pioneering works do not predict at all a sharp vanishing of the fluctuation effects at any temperature.

[20] See, e.g., M. Tinkham, *Introduction to Superconductivity*, (McGraw-Hill, New York, 1996), Chap. 4.